Multiple Roles for the Receptor Tyrosine Kinase Axl in Tumor Formation

Sacha J. Holland,[1] Mark J. Powell,[1] Christian Franci,[1] Emily W. Chan,[1] Annabelle M. Friera,[1] Robert E. Atchison,[1] John McLaughlin,[1] Susan E. Swift,[1] Erlina S. Pali,[1] George Yam,[1] Stephen Wong,[1] Joe Lasaga,[1] Mary R. Shen,[1] Simon Yu,[1] Weiduan Xu,[1] Yasumichi Hitoshi,[1] Jakob Bogenberger,[1] Jacques E. Nör,[2] Donald G. Payan,[1] and James B. Lorens[1]

[1]Rigel, Inc., South San Francisco, California and [2]University of Michigan School of Dentistry, Ann Arbor, Michigan

Abstract

A focus of contemporary cancer therapeutic development is the targeting of both the transformed cell and the supporting cellular microenvironment. Cell migration is a fundamental cellular behavior required for the complex interplay between multiple cell types necessary for tumor development. We therefore developed a novel retroviral-based screening technology in primary human endothelial cells to discover genes that control cell migration. We identified the receptor tyrosine kinase Axl as a novel regulator of endothelial cell haptotactic migration towards the matrix factor vitronectin. Using small interfering RNA–mediated silencing and overexpression of wild-type or mutated receptor proteins, we show that Axl is a key regulator of multiple angiogenic behaviors including endothelial cell migration, proliferation, and tube formation *in vitro*. Moreover, using sustained, retrovirally delivered short hairpin RNA (shRNA) Axl knockdown, we show that Axl is necessary for *in vivo* angiogenesis in a mouse model. Furthermore, we show that Axl is also required for human breast carcinoma cells to form a tumor *in vivo*. These findings indicate that Axl regulates processes vital for both neovascularization and tumorigenesis. Disruption of Axl signaling using a small-molecule inhibitor will hence simultaneously affect both the tumor and stromal cell compartments and thus represents a unique approach for cancer therapeutic development. (Cancer Res 2005; 65(20): 9294-303)

Introduction

Cancer is not a single-cell disease and tumor development involves complex reciprocal interactions among neoplastic, stromal, and immune cells (1). Cell migration is a central cellular function used by these cell types for angiogenesis, inflammation, and metastasis (2). Although it is likely that inhibitors of cell migration will complement existing cancer drugs, this possibility has been relatively neglected in the search for new cancer therapeutics.

Angiogenesis, a physiologic and strictly regulated process in healthy adults, is aberrantly induced by hypoxic tumors thus securing an adequate blood supply that feeds tumor growth and facilitates metastasis. The assembly of functional vessels requires the precise coordination of multiple cellular events and interactions (3). Compelling evidence shows that vascular endothelial growth factor (VEGF) can initiate angiogenic sprouting *in vivo*, increasing permeability and supporting endothelial cell proliferation and survival (4). Sprouting migration of activated endothelial cells is accompanied by up-regulation of integrin matrix factor receptors (e.g., $\alpha v\beta 3$ and $\alpha 5\beta 1$). Nascent endothelial tubes thus formed are stabilized by pericytes and basement membrane formation. Targeted inhibition of angiogenesis using an anti-VEGF antibody (bevacizumab) has shown efficacy in treating human cancer (5). However, as tumors frequently advanced while patients were receiving therapy, inhibition of VEGF signaling alone may not be sufficient to block neovascularization in human malignancies (6). Blocking processes complementary to those driven by VEGF may therefore be important in fully inhibiting angiogenesis in human disease.

Retroviral-based functional screening has been established as an effective, versatile, and unbiased method for identifying novel drug targets and regulators of specific cellular and/or disease processes (7). The use of retroviral expression vectors allows the efficient delivery and stable expression of complex and diverse libraries of genetic effectors (e.g., cDNAs and peptides) in a multitude of cell types including primary human cells. This allows design of screening assays in cell types that reflect physiologically relevant disease responses. We reasoned that this approach would be well suited to probing a complex and technically challenging cellular function such as cell migration.

As part of an effort to develop novel therapeutic strategies for cancer treatment, we developed a unique retroviral-based functional genetic screening protocol to discover genes that regulate cell migration in primary human endothelial cells. We identified Axl as a novel regulator of endothelial cell haptotactic migration towards the matrix factor vitronectin. Axl (UFO/ARK/Tyro7) is a receptor tyrosine kinase (RTK) that is stimulated by the ~76-kDa secreted protein Gas6 (growth arrest specific 6; refs. 8, 9). We show that Axl signaling affects multiple cellular behaviors required for neovascularization *in vitro* and regulates angiogenesis *in vivo*. Furthermore, we show that loss of Axl expression in tumor cells blocks the growth of solid human neoplasms in an *in vivo* MDA-MB-231 breast carcinoma xenograft model. This suggests a model in which Gas6-Axl signaling supports tumor-stroma interactions necessary for tumor growth and angiogenesis.

Taken together, these data indicate that Axl signaling can independently regulate neovascularization and tumor growth and thus represents a novel target class for tumor therapeutic development.

Note: J.B. Lorens is currently at the Department of Biomedicine, University of Bergen, N-5009 Bergen, Norway.

Supplementary data for this article are available at Cancer Research Online (http://cancerres.aacrjournals.org/).

Requests for reprints: Sacha J. Holland, Rigel, Inc., 1180 Veteran's Boulevard, South San Francisco, CA 94080. Phone: 650-624-1283; E-mail: sholland@rigel.com.

doi:10.1158/0008-5472.CAN-05-0993

EXHIBIT A

Materials and Methods

Antibodies. Antibodies were purchased from the following suppliers: mouse monoclonal anti-human Axl (MAB154, R&D Systems, Minneapolis, MN), rabbit polyclonal anti-actin (Cytoskeleton, Denver, CO), unconjugated anti-human CD31 (BioCare, Walnut Creek, CA), and FITC-conjugated anti-human CD31 (BD Biosciences PharMingen, Mansfield, MA). Mouse monoclonal anti-VEGFR2 was a gift from Dr. Jeanette Wood (Novartis, Basel, Switzerland). Rhodamine-conjugated *Ulex europaeus* agglutinin 1 (UEA-1) lectin was from Vector Labs (Burlingame, CA).

Cell culture. All cells were cultured at 37°C, 5% CO_2. Phoenix A cells (Dr. Gary Nolan, Stanford) were maintained in DMEM supplemented with 10% fetal bovine serum (FBS), antibiotics, and glutamine. MDA-MB-231 human breast epithelial carcinoma cells (American Type Culture Collection, Rockville, MD) were maintained in F12K supplemented with 10% FBS. Primary human umbilical vein endothelial cells (HUVEC), human dermal microvascular endothelial cells (HMVEC), and pulmonary artery smooth muscle cells (PASMC) were cultured as vendor's recommendations (Cambrex, Walkersville, MD).

Retroviral haptotaxis screen. The HUVEC green fluorescent protein (GFP)-cDNA library was prepared in the retroviral CRU5-GFP fusion vector (10). mRNA was isolated from VEGF, basic fibroblast growth factor, and epidermal growth factor–stimulated HUVECs with poly-dT magnetic beads (Dynal, Lake Success, NY) and normalized with biotinylated first strand HUVEC cDNA and streptavidin beads (Invitrogen, Carlsbad, CA). Double-stranded cDNA was synthesized using standard methods (Smart cDNA System, Clontech/BD Biosciences, Mansfield, MA) and cloned into the library vector bidirectionally using *Bst*XI adapters (Invitrogen). The complexity of the final library was 1.5×10^6. Retroviral packaging cells (Phoenix A) were transfected with the cDNA library to produce infectious virus sufficient to infect 7×10^6 subconfluent HUVEC at 10% transduction efficiency in T75 flasks. GFP-expressing HUVECS were sorted by fluorescence-activated cell sorting (FACS) and replated. The following day, the cells were harvested and migrated thrice in 75-mm Boyden chambers (Transwell, Corning-Costar, Acton, MA) coated on the underside with 15 μg/mL vitronectin (Chemicon, Temecula, CA). Each migration was conducted for 3 hours. Nonmigrating cells were harvested with 0.05% Trypsin for 90 seconds at 37°C and remigrated. The cells were infected with wild type Moloney murine leukemia virus (MMTV, American Type Culture Collection) before the third migration step to produce library clone viruses from the enriched nonmigratory cell population. The final selected nonmigratory HUVEC population was plated and library viruses were harvested the following day and used to infect PG13 packaging cells at a low multiplicity of infection (0.5%). Single GFP^+ PG13 cells were arrayed into microtiter plates by FACS. cDNA inserts were isolated by reverse transcription-PCR (RT-PCR, Clontech/BD Biosciences) from purified retrovirus (12). To confirm the library insert phenotype, naive HUVECs were transduced using supernatants from each PG13 clone. GFP-expressing cells were purified by FACS and tested in individual haptotaxis assays (see below).

Small interfering RNA design and transfection. Luciferase control (GL2), VEGFR2 (D-003148-05), and custom small interfering RNA (siRNA) oligos were purchased from Dharmacon (Lafayette, CO). siRNA sequences (Supplementary Table 1) were designed according to established criteria and examined to ensure minimal homology with other sequences. For siRNA transfection, 60,000 HUVECs were plated per well in a six-well plate. The following day, cells were transfected with 3.2 μg siRNAs using Oligofectamine reagent in Opti-MEM (both Invitrogen) for 4 hours after which 3× volume of culture medium containing 6% FBS was added.

Constructs. The shRNA vector (EFS-U3/U6) was derived from the TRA retroviral vector (10). The EFS-U3/U6 vector comprises retroviral elements required for stable integration into the genome of infected cells, a modified U6 RNA promoter (−230 to +1) and terminator (TTTTT) embedded into the *Nhe*I site of the TRA vector 3′ long terminal repeat for conditional expression of hp-siRNA and an internal EF1-α expression cassette (11) that drives expression of a destabilized version (COOH-terminal PEST sequence) of the *Renilla* GFP (dsRMG) for independent monitoring of transfection/infection efficiencies. Specific shRNA vectors were created by PCR. COOH-terminally *myc*-tagged Axl cDNA (480-3140) was expressed from an IRES-GFP vector (10) derivative where GFP is replaced with *Renilla* GFP.

Transfection/retroviral infection. Phoenix A cells were transfected using the calcium phosphate method (12). Approximately 30 hours after transfection, the medium was changed to growth medium for the cells to be infected, supplemented with 10% FBS. Infectious supernatant was collected ~48 hours after transfection. Target cells were exposed to supernatant containing 5 μg/mL protamine sulfate for 6 hours to overnight before being returned to regular growth medium.

Taqman. Total RNA was isolated using RNeasy Mini Kit (Qiagen, Valencia, CA) and quantified using Ribo Green Quantification kit (Molecular Probes, Eugene, OR). Human Gas6 primers and probe were designed using Primer Express software: sense primer, ATGTGGCAGACAATCTCTG; reverse primer, ACAGCATCCCTGTTGACCT; probe, AGCTGGCGCGG-AATCTGGTCA. Reactions were run using a one-step RT-PCR kit (Qiagen) in an ABI Prism 7900HT sequence analyzer. An 18S rRNA reaction kit (ABI, Foster City, CA) was used as the reference/loading control reaction. Data was normalized to 18S rRNA and plotted as percentage of luciferase control.

Western blot. Cells were lyzed in PLC lysis buffer containing 1% Triton X-100 (13). Protein concentrations were determined using the bicinchoninic acid protein assay kit (Pierce, Rockford, IL) and equalized. SDS-PAGE and Western blotting were carried out according to standard procedures.

Boyden chamber haptotaxis assay. Migration assays were done 48 hours after siRNA transfection, or 1 to 2 days after sorting of infected populations. The undersides of 8 μm 24-well Transwell filters (Costar) were coated with 15 μg/mL vitronectin (Chemicon). Six replicate wells were run per sample. The following day, unbound vitronectin was eluted in migration medium [0.5% bovine serum albumin (BSA, Sigma, St. Louis, MO) in EGM-2 medium (Cambrex)]. Migration medium (500 μL) was added into the lower chamber. HUVECs resuspended in migration medium at 2,000 cells/300 μL per well were added to the upper chamber. Cells were allowed to migrate for 3 hours at 37°C after which they were removed from either the upper or lower surface of the membrane (three wells each) using a cotton swab. Following fixation in 3.7% formaldehyde, swabbing was repeated and nuclei were stained using 2 μg/mL 4′,6-diamidino-2-phenylindole. Cells remaining on the upper (nonmigrated cells) or lower (migrated cells) surface of the membrane were imaged using a Cellomics Arrayscan instrument and processed using ImagePro software. Migration is presented as mean haptotactic index (% nonmigrated, control / % nonmigrated, test) ± SD: 1, no effect; >1, enhanced migration; <1, retarded migration. Representative examples of at least two replicate experiments are shown. Statistical analysis was done using the χ^2 test.

Proliferation assay. Cells were seeded sparsely in six-well dishes, infected with retroviral supernatants, and maintained in complete endothelial cell medium. The percentage of infected, GFP-positive cells in the population was monitored at regular intervals by FACS. Cells were passaged during the course of the experiment as necessary to keep them subconfluent. Data was analyzed using FlowJo software. The relative number of GFP-positive cells for all samples at the beginning of the experiment (day 3) was set to 100%. Subsequent changes in relative % GFP over time were normalized to the in-day vector control value.

Coculture assay. Early-passage HUVECs (≤p6) were mixed 1:10 with PASMC in HUVEC growth medium (EGM-2) and seeded onto collagen-coated (Sigma) LabTekII chamber slides (Nalge Nunc, Rochester, NY). Medium was replaced every 2 days. Five days after seeding, the cocultures were washed in PBS, fixed using −20°C/70% ethanol at room temperature for 15 minutes, blocked in PBS + 5% BSA, and stained using FITC-conjugated anti-CD31 antibodies or Rhodamine-conjugated UEA-1 lectin (1:200) to reveal endothelial cell tubes. Cultures were photographed and mean tube formation over 16 images covering an entire representative well was quantified using ImagePro software. Representative examples of at least two replicate experiments are shown. Statistical analysis was done using the *t* test.

***In vivo* angiogenesis assay.** HMVECs were infected with shRNA vectors and GFP-positive cells were enriched by FACS. Poly L-lactic acid (PLLA) sponge matrices (5 × 5 × 1 mm) were seeded with 700,000 sorted HMVEC

cells in a 1:1 mixture of EGM-2 MV and Matrigel (BD Biosciences). Up to four sponges were implanted s.c. in female CB-17 severe combined immunodeficient (SCID) mice according to Nör et al. (14). Sponges were harvested after 14 days for biochemical or immunohistochemical analysis.

To specifically label perfused human endothelial cells in the sponges, 200 μL of rhodamine-conjugated UEA-1 lectin (1 μg/μL in sterile 0.9% NaCl) was injected into the tail vein 30 minutes before sacrifice. Excised sponges were homogenized using a handheld mincer (Biospec Products, Inc., Bartlesville, OK) in 200 μL of modified radioimmunoprecipitation assay buffer. Fluorescence in filtered (0.45-μm GHP syringe filter, Pall-Gelman Corp., Inc., East Hills, NY) supernatant was quantified on a Fluorskan machine with a 530/590-nm excitation/emission filter pair and normalized to plasma lectin content. Tie-2 levels present in sponge lysates (100 μL) were measured using a human Tie-2 ELISA (R&D Systems) and normalized to protein content.

Statistical analysis between groups was done using the Mann-Whitney rank sum test.

Xenograft assay. MDA-MB-231 cells were infected with shRNA vectors and GFP positive populations were enriched to 98% to 100% by FACS. RNA interference (RNAi)–mediated knockdown of cell surface Axl expression was confirmed on the day of implantation. Cells (1×10^7) were injected in 0.2 mL of F12K medium + 10% FBS/high concentration Matrigel (1:1 ratio, BD Biosciences) into the right flank of female CB-17 SCID mice. Animals in which tumors measured at least 0.3 to 0.5 cm were selected for the study. Tumor volume [V = (tumor length × tumor width^2) / 2] was measured every 2 to 3 days for 30 days, or until it reached a volume of 2,000 mm^3. Tumor growth was expressed as V/V_o, where V = tumor volume and V_o = initial volume of tumor. Mean V/V_o and SDs were calculated using Labcat Software. Statistical analysis between groups was done using the t test.

Immunohistochemistry. Staining reagents were from BioCare. Heat-induced epitope retrieval was done on 4 μm paraformaldehyde/formalin-fixed, paraffin-embedded tissue sections using Medical Decloaking Chamber in Borg high-pH buffer for 2 minutes followed by rinses in Hot Rinse Solution to remove residual paraffin. Nonspecific staining was eliminated using SNIPER blocking reagent. Primary antibody (mouse monoclonal anti-human CD31; 1:50 or mouse monoclonal anti-human Axl, 1:100) incubations were followed by biotinylated goat anti-mouse/rabbit secondary (BioCare) and then alkaline phosphatase or horseradish peroxidase–conjugated streptavidin. Development was done according to the manufacturer's instructions. Slides were counterstained with hematoxylin, mounted, and coverslipped. Brightfield pictures were taken using a Nikon Eclipse 400 microscope with a Spot Insight QE imaging system.

Results

Genetic screen to identify modulators of vitronectin haptotaxis. We established a retroviral-based functional screen to select for genes that regulate endothelial migration (Fig. 1*A*). Similar screens, based on cell survival, proliferation, and surface marker expression, have been done in transformed cell lines (7, 15–20). To institute a physiologically relevant screening assay, we used early-passage primary HUVECs. A GFP-fused HUVEC cDNA library was constructed in a retroviral vector. The GFP

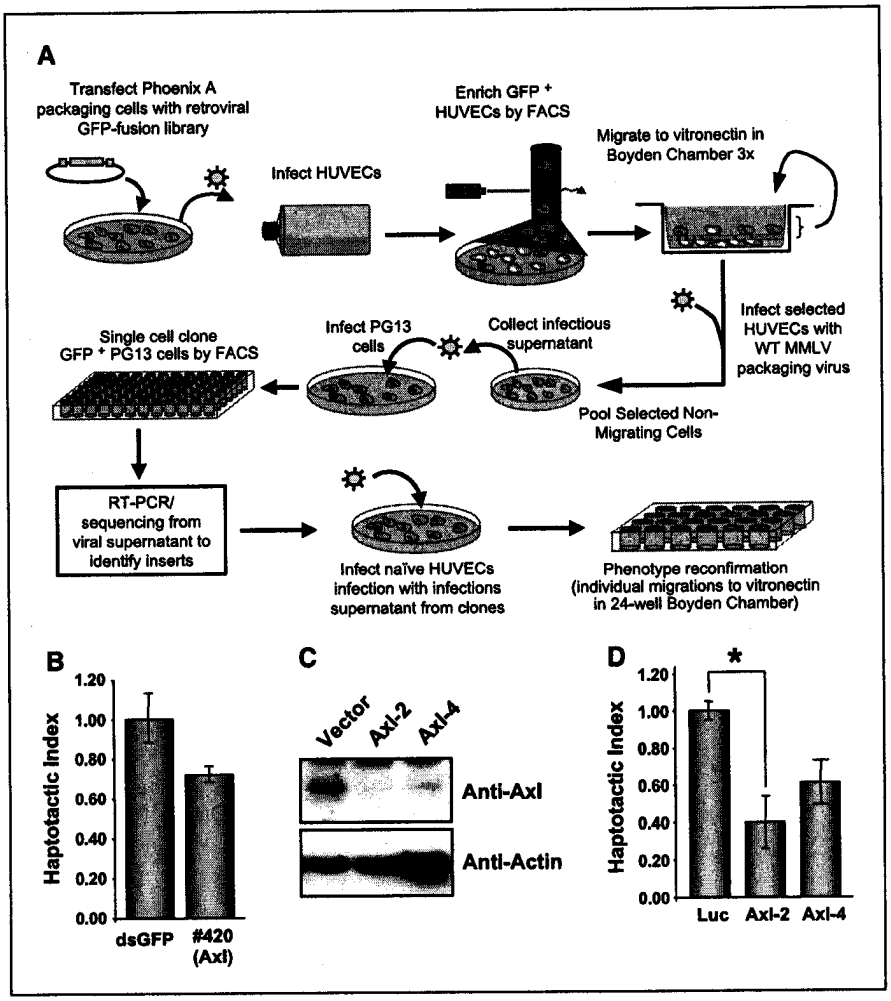

Figure 1. Antisense cDNA effector corresponding to Axl was identified in a retroviral-based functional screen for inhibitors of endothelial cell haptotaxis. *A*, haptotaxis screen protocol. Phoenix A packaging cells were transfected with a retroviral GFP-cDNA fragment library. Retrovirus-containing medium was collected and used to infect HUVECs. The infected, GFP-expressing HUVEC population was enriched by FACS and subjected to three rounds of migration in Boyden chambers coated on the underside of the membrane with 15 μg/mL of vitronectin. To rescue the library inserts, selected HUVECs were infected with WT virus and infectious supernatant was used to infect PG13 packaging cells. PG13 clones containing a single library insert each were arrayed in microtiter plates as single cells by FACS and expanded. Library virus RNA from individual PG13 clones was used as a template for RT-PCR to isolate cDNA inserts. Retroviruses from selected clones were used to infect naive HUVECs and individual migration experiments were carried out to reconfirm insert phenotypes. *B*, haptotaxis towards vitronectin. HUVECs were infected with virus from PG13 clone #420 or control vector. GFP-positive cells were enriched by FACS and subjected to haptotaxis towards 15 μg/mL of vitronectin. Expression of GFP-Axl antisense cDNA fragment reduced haptotaxis compared with control. *Columns*, mean haptotactic index; *bars*, ±SD. % Nonmigrated, control / % nonmigrated, test: 1, no effect; >1, enhanced migration; <1, retarded migration. *C-D*, siRNAs targeting Axl inhibit endothelial cell haptotaxis. HUVECs were transfected with a control siRNA targeting luciferase or two independent siRNAs targeting different sequences within the endogenous Axl message (Axl-2 and Axl-4). After 48 hours, cells were assayed (*C*) for target knockdown by Western blot (showing reduction of Axl expression to near background levels) or (*D*) haptotaxis towards 15 μg/mL of vitronectin. *, $P < 0.001$ (χ^2 test) compared with control.

moiety stabilizes fusion proteins, reveals subcellular localization, and facilitates identification of vector-infected cells. Furthermore, the bidirectional cloning strategy yields potential antisense effectors (21). This library was introduced into HUVECs at a low infection rate (10%) to avoid multiple viral integrations per cell. The infected, GFP-expressing cell population was enriched by FACS and cells with impaired haptotactic motility towards 15 μg/mL vitronectin were selected by three rounds of migration in a modified Boyden chamber assay (see Materials and Methods).

As the HUVEC life span is limited, we developed a technique to rescue genetic library information from the selected cells and transfer it to a more robust, transformed cell type. Nonmigrating HUVECs were infected with wild-type (WT) MMLV to package resident library viruses (15). Virion-containing medium was harvested and used to infect the NIH3T3-derived PG13 packaging cell line at a very low infection rate to ensure a single infection per cell. Single-cell PG13 clones were arrayed in microtiter plates by FACS and expanded. Library inserts were isolated by PCR using the retroviral DNA as the template and sequenced.

Two hundred fifty four independent library inserts were identified. Library clone #420 encoded a fragment from the COOH-terminal region of the RTK Axl (nucleotides 2884-2964), which was oriented in the reverse direction indicating that it may function as an antisense effector.

Genetic effectors targeting Axl impair vitronectin haptotaxis. To reconfirm that the isolated clone #420 virus could reproduce the phenotype selected for in the screen, retroviral supernatant from clone 420 was used to infect naive HUVECs. GFP-expressing cell populations were enriched by FACS and assayed by migration towards 15 μg/mL of vitronectin. HUVECs infected with the Axl genetic effector indeed showed reduced haptotactic migration towards vitronectin (Fig. 1*B*).

We used siRNA-mediated silencing to independently verify that Axl knockdown could inhibit vitronectin haptotaxis. Compared with HUVECs transfected with a control siRNA-targeting luciferase, those transfected with either of two independent siRNAs targeting Axl (Fig. 1*C*) phenocopied the effect of the Axl antisense screening insert and exhibited reduced migration towards vitronectin (Fig. 1*D*). Furthermore, GFP-expressing retroviral vectors designed to produce shRNAs corresponding to these Axl-silencing sequences generated a similar reduction in haptotaxis (data not shown). Axl expression in HUVECs is thus required for haptotaxis towards vitronectin.

Axl regulates human umbilical vein endothelial cell proliferation. An important characteristic of angiogenic endothelial cells is their high proliferative capacity. As Gas6 is a weak mitogen in some cell types, we asked whether Axl signaling regulates HUVEC proliferation. HUVECs infected with Axl shRNA vectors or a positive control construct expressing the cell cycle inhibitor p21 (22) exhibited a marked growth disadvantage compared with controls (Supplementary Fig. 1). Furthermore, although we did not detect significant apoptosis in Axl shRNA-expressing cell populations under the assay conditions, Axl silencing also reduced DNA replication as assayed by bromodeoxyuridine incorporation (data not shown). Taken together, these data show that Axl expression is important in driving HUVEC proliferation.

Axl knockdown impairs endothelial tube formation *in vitro*. We next addressed whether Axl regulates endothelial tube formation. To mimic the complex matricellular environment encountered by angiogenic endothelial cells *in vivo*, we designed a HUVEC/primary PASMC coculture branching morphogenesis/tube formation assay (Fig. 2*A*). Endothelial morphogenesis in this assay is VEGF dependent and proliferation independent (see Supplementary Fig. 2).

HUVECs were transfected with Axl siRNAs and seeded into a coculture assay (Fig. 2*B*). Axl knockdown was similar to that in Fig. 1*C* (data not shown). Total tube formation, fiber length, and branching were reduced by at least ~50 % in HUVECs transfected with Axl siRNAs (Fig. 2*B*, *ii*, *iii*, *v*, and *vi* and *C*; data not shown) compared with those transfected with the luciferase control siRNA (Fig. 2*B*, *i* and *iv* and *C*). These results show that Axl is involved in the regulation of endothelial tube morphogenesis.

Endothelial cell Gas6 expression and Axl catalytic activity are required for regulation of proangiogenic processes. We next asked whether ligand-stimulated Axl catalytic activity is required for its proangiogenic functions. HUVECs synthesize the Axl ligand, Gas6 (23). Two independent siRNAs designed to target Gas6 depressed HUVEC Gas6 message levels and reduced HUVEC haptotaxis towards vitronectin compared with controls (Supplementary Fig. 3). Gas6 silencing thus phenocopies the effect of Axl knockdown on vitronectin haptotaxis.

We next focused on the catalytic activity of Axl. Overexpression of WT Axl in HUVECs (Fig. 3*A*) induced a growth advantage relative to controls (Fig. 3*B*). Conversely, overexpression of a catalytically inactive Axl mutant (AxlKD; $K_{567}E$ substitution; ref. 24; Fig. 3*A*) conferred a ~30% growth disadvantage over the course of the assay (Fig. 3*B*). Lastly, sorted, GFP-positive WT Axl or GFP-infected HUVECs were seeded into a coculture assay. Overexpression of WT Axl led to ~40% increase in the number of endothelial cell tubes formed compared with control vector (Fig. 3*C*, *ii* and *v* and *D*). In contrast, overexpression of AxlKD did not enhance tube morphogenesis (Fig. 3*C*, *iii* and *vi* and *D*). Similar trends were noted for fiber length and branching (data not shown). The autocrine/paracrine ligand-induced kinase activity of Axl therefore controls several distinct proangiogenic processes and thus represents an attractive target for small-molecule inhibition.

Axl knockdown impairs blood vessel formation and function in a mouse angiogenesis model. Because our observations suggest that Axl signaling may regulate angiogenesis *in vivo*, we investigated this possibility using the SCID mouse model of human angiogenesis (Fig. 4*A*; ref. 14).

Primary HMVECs were infected with the Axl shRNA vectors, an shRNA vector that silences VEGFR2 or the luciferase shRNA control vector. FACS-enriched GFP-expressing cells were mixed with Matrigel, seeded into PLLA scaffolds, and subsequently implanted into SCID mice. Over 14 to 22 days, the human endothelial cells form vessels that anastamose with recruited mouse vasculature, connecting them to the mouse circulation. HMVECs not incorporated into vessels typically undergo apoptosis by around 14 days (J.E. Nör, data not shown). Vessel formation was analyzed 14 days after implantation by measuring human Tie-2 levels in implant lysates by ELISA. In implants containing HMVECs infected with VEGFR2 or Axl shRNA vectors, human Tie-2 levels were reduced by 42% and over 50%, respectively (Fig. 4*C*, *i*) indicating that Axl silencing impairs neovascularization.

Fluorescent UEA-1 lectin, which binds specifically to human endothelial cells, was injected into the mouse bloodstream before sacrifice. The relative fluorescence in implant lysates compared with mouse plasma provides a measure of functional circulation in

the human neovasculature. Figure 4*C* (*ii*) shows a marked reduction (77% for Axl-2 and 58% for Axl-4) in lectin fluorescence (i.e., implant perfusion) in Axl shRNA samples compared with controls, indicating a functional impairment in human neovessels lacking Axl expression.

Vessel morphology was assessed by anti-human CD31 staining of implant sections. Control vector–infected HMVECs formed small capillaries with obvious lumens (Fig. 4*D, i, arrow*). Moreover, developing blood vessels seem to have fused normally to form larger vessels (Fig. 4*D, ii, arrow*). In contrast, vessels generated by HMVECs infected with Axl shRNA vectors seem consistently smaller than controls and lack patent lumens (Fig. 4*D*, *iii* and *iv*).

These data show that Axl expression in endothelial cells is important for the formation of functional blood vessels *in vivo*.

Inhibition of Axl expression reduces growth of MDA-MB-231 breast carcinoma cells in a xenograft assay. Axl is overexpressed in a large variety of human tumors and has transforming activity in murine NIH3T3 and 32D cells (25–27), suggesting the possibility that Axl may act as an oncogene. However, functional evidence that Axl can drive the growth or progression of human tumors *in vivo* has thus far not been forthcoming.

The human breast tumor line, MDA-MB-231, which expresses high levels of Axl (Supplementary Fig. 4; ref. 28), was infected with Axl shRNA vectors. We did not detect significant changes in the proliferation or apoptosis of Axl-shRNA-infected MDA-MB-231 cells in culture compared with controls (data not shown). GFP-positive cells were enriched by FACS and implanted s.c. into SCID mice. Compared with vector controls, MDA-MB-231 cells infected with Axl shRNA vectors showed a markedly impaired ability to grow as xenografts in immunocompromised mice (Fig. 5*B*). The extent of inhibition correlated with the degree of Axl knockdown, assayed by immunostaining for Axl protein in tumor sections harvested at the end of the study (Fig. 5*C*). Whereas the mechanism underlying these observations in xenografts is not understood at present, these results show that, in addition to regulating angiogenesis, Axl plays a key role in driving the growth of human tumor cells *in vivo*.

Discussion

Inhibitors of cell migration, a basic cellular behavior central to the complex crosstalk between tumor and stromal compartments necessary for malignant progression, will likely complement existing antitumor therapeutics. Using a retroviral-based phenotypic-screening strategy to discover regulators of haptotactic migration in primary human endothelial cells, we identified the

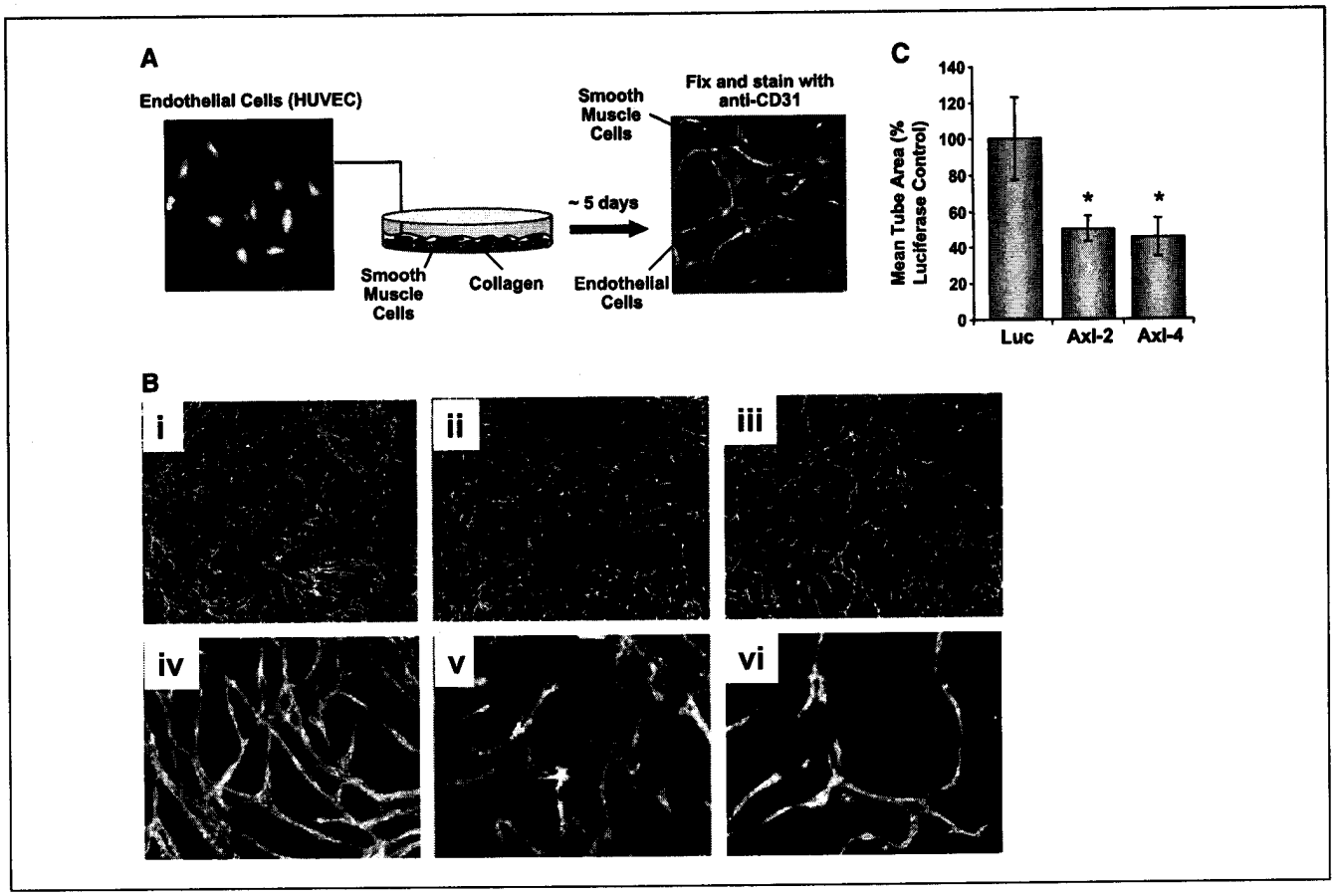

Figure 2. Axl inhibition blocks endothelial tube formation. *A*, endothelial cell/SMC coculture system. A 1:10 mixture of HUVECs and PASMCs were seeded onto collagen-coated tissue culture wells in HUVEC medium. After 5 days, endothelial tubes were fixed and visualized by staining with FITC-conjugated anti-CD31 antibodies or Rhodamine-labeled UEA-1 lectin. *B*, Axl siRNAs reduce tube formation. HUVECs were transfected with siRNAs targeting Axl or control siRNA targeting luciferase. After 24 hours they were seeded into the coculture assay as in (*A*). Axl siRNAs reduce endothelial tube formation. Magnification, 4× (*i-iii*) and 10× (*iv-vi*). *i* and *iv*, luciferase siRNA control; *ii* and *v*, Axl-2; *iii* and *vi*, Axl-4. *C*, quantification of tube formation. *Columns*, mean area per field covered (quantified using ImagePro) by endothelial tubes in images from (*B*); *bars*, ±SD. *, $P < 0.001$ (*t* test) compared with control.

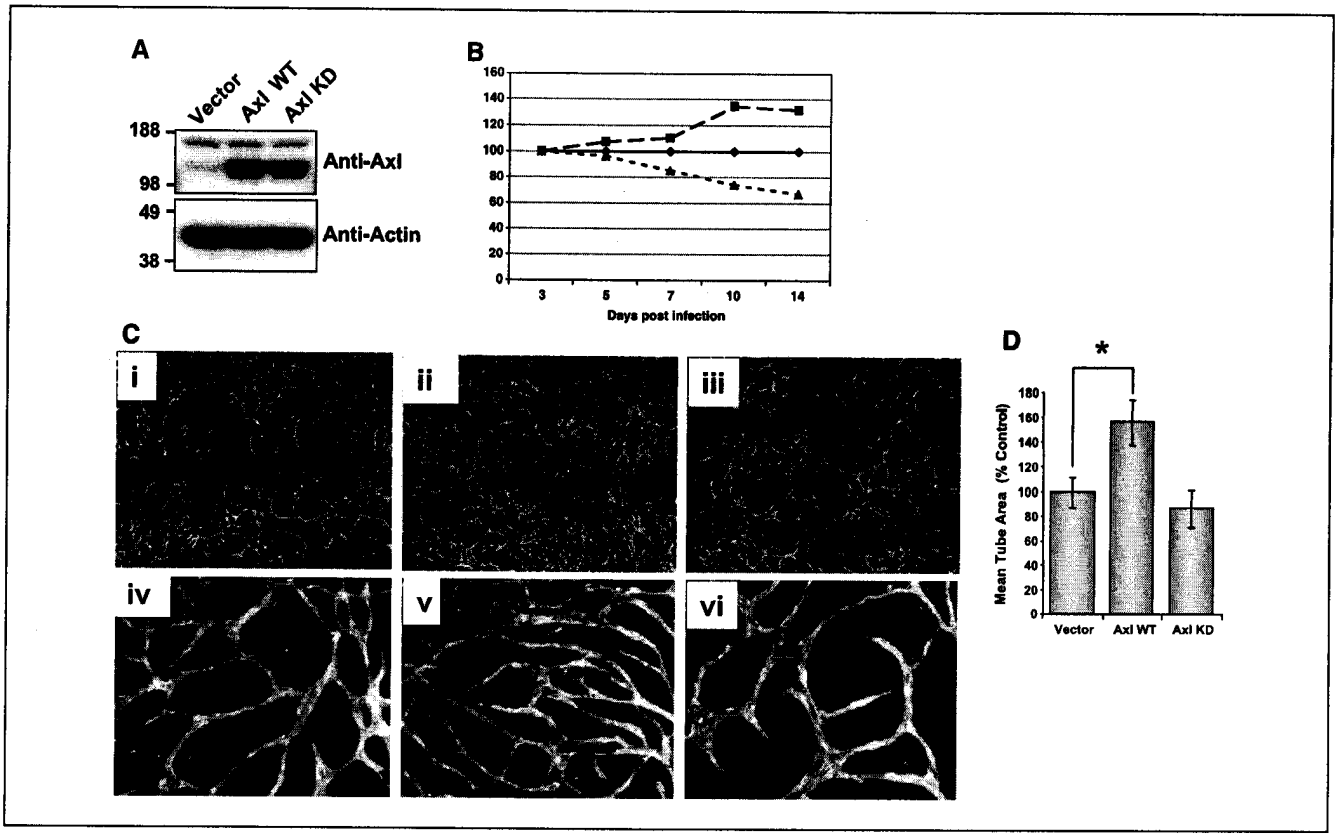

Figure 3. Axl catalytic activity is required for regulation of pro-angiogenic phenotypes. *A* and *B*, Axl catalytic activity regulates HUVEC proliferation. *A*, expression of Axl in FACS-enriched GFP + HUVEC populations infected with wild type Axl, AxlKD, or control vector was assayed by Western blot. *B*, % GFP in the infected populations was monitored over time by FACS as in Supplementary Fig. 1. AxlWT (*broken dashed line, squares*) increases and AxlKD (*broken dotted line, triangles*) reduces HUVEC growth compared with control vector (*solid line, diamonds*). Initial absolute % GFP on day 3 was Vector, 69.3%; AxlWT, 43.2%; and AxlKD, 60.3%. *C* and *D*, Axl catalytic activity regulates endothelial tube formation. *C*, sorted, GFP-positive infected populations were seeded into the coculture as in Fig. 2. Axl AxlWT enhances endothelial cell tube formation, whereas Axl KD does not. Magnification, 4× (*i-iii*) and 10× (*iv-vi*). *i* and *iv*, Vector control; *ii* and *v*, AxlWT; *iii* and *vi*, AxlKD. *D*, *columns*, mean area per field (quantified using ImagePro as in Fig. 2*C*) covered by endothelial tubes in images from (*C*); *bars*, ±SD. *, $P < 0.001$ (*t* test) compared with vector.

RTK Axl as a key modulator of multiple endothelial cell processes (proliferation, migration, endothelial cell survival, and tube formation) required for angiogenesis and tumor growth.

The receptor tyrosine kinase Axl was first identified from the DNA of chronic myelogenous leukemia patients due to its transforming activity *in vitro* (25, 26). Expression of Axl is detected in many cell types but is prominent in the vasculature (in both endothelial cells and vascular SMCs, VSMC) and in cells of the myeloid lineage (29–31). Axl and its two close relatives Mer/Nyk and Sky (Tyro3/Rse/Dtk) all bind and are stimulated to varying degrees by Gas6 (8, 9). Axl signaling in culture protects cells from serum starvation– or tumor necrosis factor-α-induced apoptosis and mediates ligand-induced chemotaxis and cell differentiation (24, 31–33). However, $Axl^{-/-}$ mice exhibit no overt phenotype and the physiologic function of Axl *in vivo* is not clearly established (34). The overexpression of Axl and/or its ligand, Gas6, has been reported in a wide variety of solid human tumor types (ref. 35 and references therein) and myeloid leukemias (30). Axl signaling is also functionally implicated in the response to vascular injury and kidney disease (29, 36). Axl may thus potentially represent a therapeutic target for diverse pathologic conditions.

Our data suggest that Axl acts as a central facilitator of endothelial cell activation. Axl may support pathologic neovascularization as impaired developmental angiogenesis has not been reported in $Axl^{-/-}$ mice. Axl and Gas6 are coexpressed in endothelial cells and silencing of either gene impairs vitronectin haptotaxis. Thus, a constitutive autocrine/paracrine signaling loop may exist in these cells (ref. 37; data not shown). Axl may modulate activated endothelial cell functions through one of several possible mechanisms: (a) Axl signaling in endothelial cells may support the activated state, potentially by altering gene expression, thus maintaining a proliferative, motile phenotype. Axl inhibition may therefore alter the angiogenic balance, driving endothelial cells towards a more quiescent, nonmotile, differentiated state. (b) Axl signaling modulates integrin function. Angelillo-Scherrer et al. recently showed that Gas6-dependent signaling results in phosphorylation of β3 integrin in platelets (38) resulting in defective αIIbβ3-dependent "outside-in" signaling in $Axl^{-/-}$ platelets. Similar crosstalk has been described between growth factor receptors (e.g., VEGFR2 and FGFR) and integrins (e.g., αvβ3 and αvβ5; ref. 39). Integrin-mediated substrate adhesion is required for cell migration, proliferation, and survival of growth factor–stimulated cells. Thus, blocking Axl signaling may alter the function of certain integrins necessary for the growth, migration, and survival of endothelial cell and tumor cells. (c) Constitutive Gas6 stimulation may maintain the steady state activity of Axl effectors such as Rac and Akt (40, 41) that

control matrix- and chemoattractant-induced cell motility. The defective lumen morphology observed in vessels lacking Axl may reflect regulation of the Rho/Rac-dependent fusion of intracellular vacuoles thought to control lumen generation (42, 43). Akt is a positive regulator of angiogenesis and is central to both Gas6- and VEGF-induced endothelial cell survival (41, 44). Moreover, the pivotal role of Akt in tumor development is well documented (45).

Axl knockdown diminished vitronectin haptotaxis, proliferation, and blunted endothelial cell tube morphogenesis *in vitro*. Conversely, overexpression of WT Axl but not AxlKD enhanced endothelial cell growth and tube formation. Whereas we cannot at present rule out a contribution from homophilic adhesive interactions via the ligand-binding domain (46), these observations show the kinase dependency of proangiogenic Axl signaling and imply that this process is a classic target for small-molecule drug inhibition.

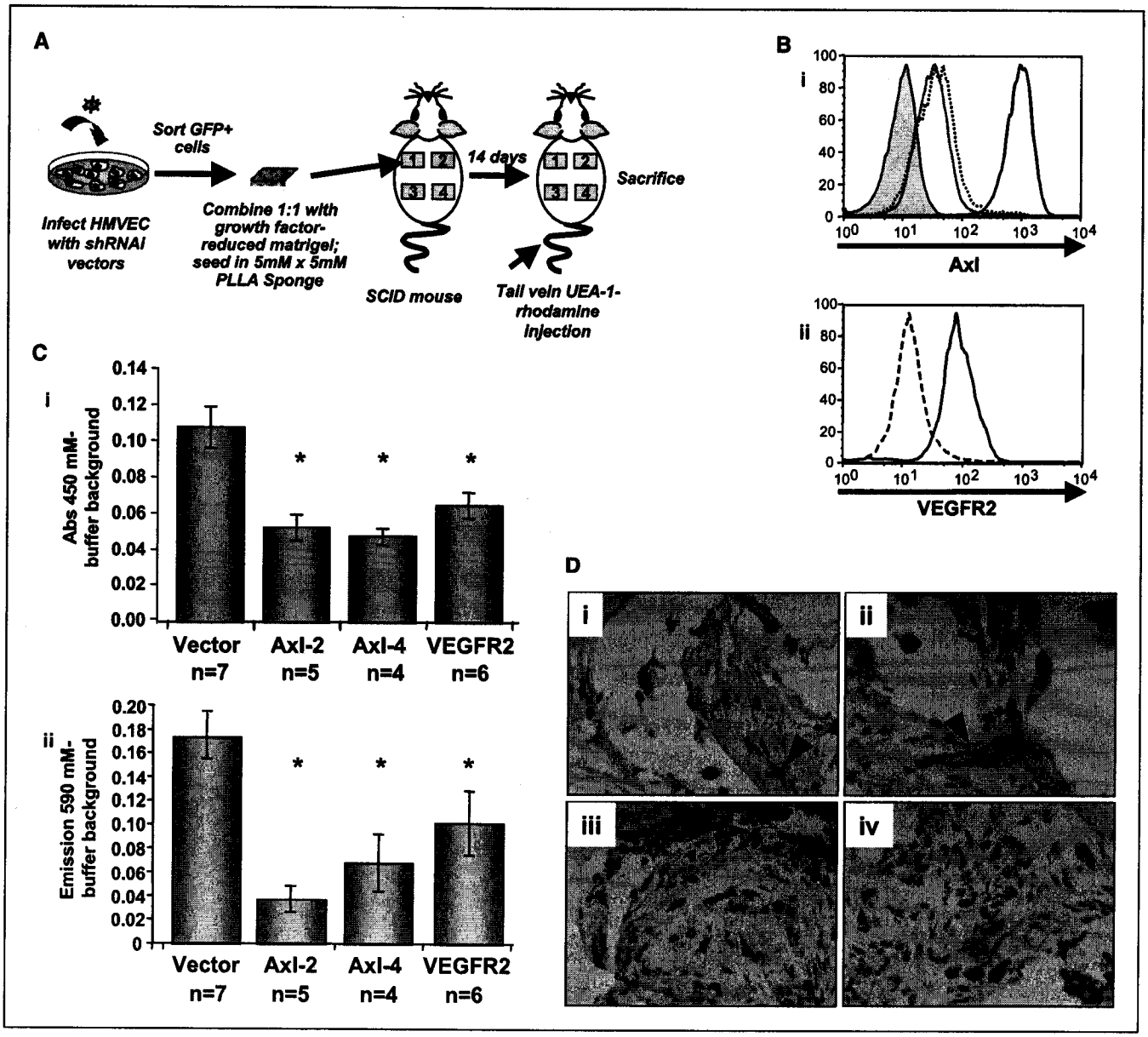

Figure 4. Axl knockdown in endothelial cells inhibits angiogenesis *in vivo*. *A*, experimental protocol. HMVEC cells were infected with two independent Axl shRNA vectors, VEGFR2 shRNA vector, or luciferase shRNA vector control. GFP-positive populations were enriched by cell sorting, mixed with growth factor–reduced Matrigel, and seeded into PLLA scaffolds. Scaffolded HMVECs were implanted s.c. into SCID mice and harvested after 14 days *in vivo*. Thirty minutes before harvest, Rhodamine-conjugated UEA-1 lectin was administered by tail vein injection. *B*, FACS analysis of infected cells before implantation. *i*, Axl expression in vector infected (*solid line*; isotype control, *filled*) and Axl-2 (*solid grey line*) and Axl-4 (*broken line*) shRNA infected cells. A ~97% reduction in Axl surface expression was achieved relative to vector control. *ii*, VEGFR2 expression in vector-infected cells (*solid line*) and VEGFR2 shRNA–infected cells (*broken line*). A ~92% reduction in VEGFR2 surface expression was achieved relative to vector control. *C*, quantification of angiogenesis in sponges. *i*, total human endothelial cell content was quantified using human Tie-2 ELISA on sponge lysates. $A_{450\ nm}$ for an implanted blank sponge control = 0.018. *, $P \leq 0.05$ compared with vector. *ii*, human endothelial cells in functional vessels perfused with mouse blood quantified by absorbance at 590 nm in sponge lysates (Rhodamine-conjugated UEA-1 lectin). Emission 590 nm for a blank sponge control = 0.017. *, $P \leq 0.05$ compared with vector. *D*, anti-CD31 staining of human vessels in sponges. *i* and *ii*, vector control; *iii* and *iv*, Axl-2. *i/iii* and *ii/iv*, samples from two independent mice.

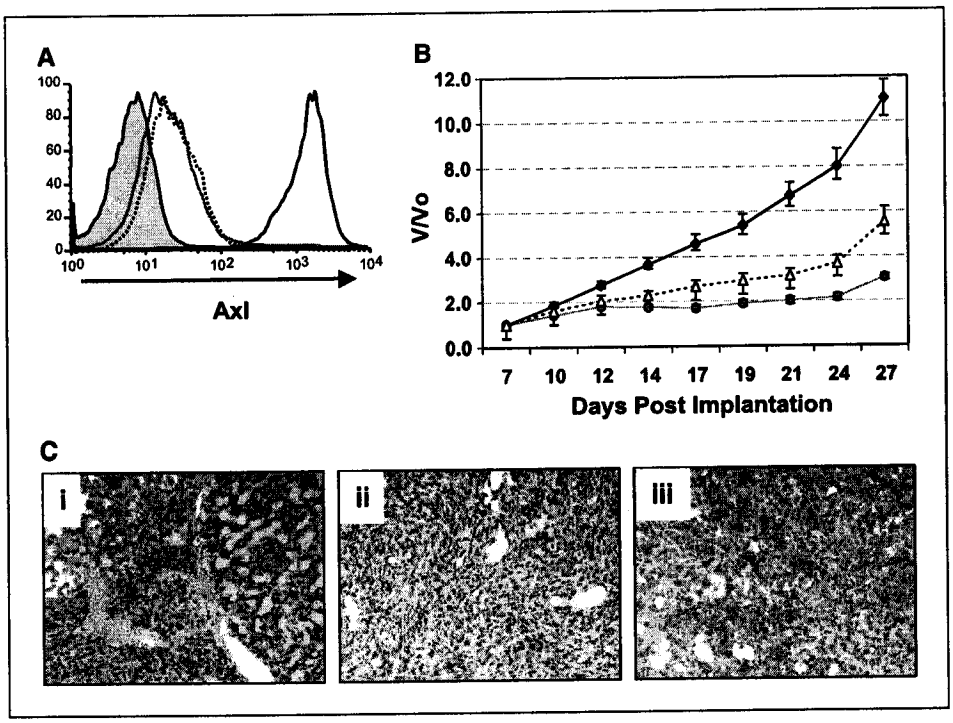

Figure 5. Axl knockdown in human tumor cells inhibits xenograft growth *in vivo*. MDA-MB-231 cells were infected with two independent Axl shRNA vectors or shRNA vector control. GFP-positive populations were enriched by cell sorting, and injected s.c. into SCID mice (Vector; Axl-4, $n = 13$; Axl-2, $n = 12$). Xenograft growth was measured over a 27-day period. *A*, FACS analysis of infected cells before implantation. *i*, Axl expression in vector-infected cells (*solid line*; isotype control, *filled*), Axl-2-infected cells (*solid grey line*) and Axl-4 shRNA–infected cells (*broken line*). A ~97% reduction in Axl surface expression was achieved relative to vector control. *B*, xenograft growth. Growth of MDA-MB-231 cells infected with vector control (*filled diamonds*), Axl-2 (*filled circles*), and Axl-4 (*triangles*) in xenograft assay (V/V_0: volume/initial volume). Slopes of Axl-2 and Axl-4 curves were significantly different from vector ($P < 0.001$, *t* test). *C*, expression of Axl in xenografts after 27-day growth. Tumor sections were stained with anti-Axl antibodies. Axl staining is reduced in Axl-2 (*ii*) and Axl-4 (*iii*) shRNA samples compared with vector control (*i*). Magnification, 20×.

Gallicchio et al. recently reported that Gas6 antagonizes VEGFR2-dependent angiogenic processes (47). Low Gas6 concentrations (~0.01 ng/mL) blocked VEGFR2 phosphorylation and VEGF chemotaxis, whereas high concentrations (>20 ng/mL) had little effect and >40 ng/mL Gas6 impaired tube formation in the Matrigel assay (47). We have not studied VEGF-induced chemotaxis; however, tube formation in endothelial cell/SMC cocultures is VEGF-dependent (see Supplementary Information), although both endothelial cells and SMCs express Gas6 (data not shown; refs. 29, 37). Axl knockdown impairs endothelial tube formation and overexpression of WT but not catalytically inactive Axl enhances endothelial cell tube morphogenesis. Furthermore, Axl silencing in an *in vivo* angiogenesis model produces an inhibitory phenotype similar to VEGFR2 knockdown. To reconcile these observations, one could address whether Axl silencing blocks Gas6-mediated VEGFR2 inhibition.

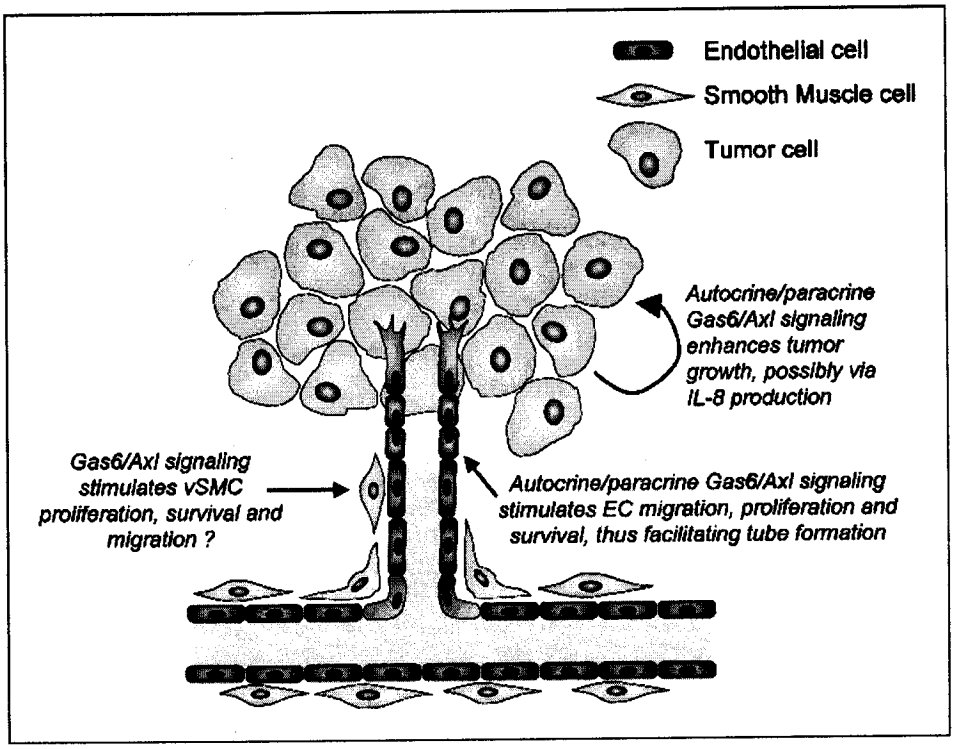

Figure 6. Role of Axl signaling in angiogenesis tumor growth. We and others have shown that (autocrine/paracrine) Gas6/Axl signaling stimulates endothelial cell (*EC*) migration, proliferation, and survival thus facilitating tube formation. Axl expression is high in many human tumors and contributes to driving tumor growth in a xenograft assay using human MDA-MB-231 breast cancer cells, potentially via up-regulation of IL-8. Axl/Gas6 signaling also regulates migration, proliferation, and survival in SMCs. Inhibition of Axl catalytic activity could therefore potentially block tumor growth by acting on three distinct cellular targets.

Pronounced Axl expression has been documented in a variety of human cancers (ref. 35 and references therein). Furthermore, Axl possesses transforming activity in NIH3T3 and 32D cells (25–27). In endothelial cells, Axl controls diverse processes including growth, survival, migration, and morphologic differentiation linked to the proliferative and invasive changes required for angiogenic activation (31, 37, 41). These mechanisms are also central to tumor formation and progression *in vivo*. Although no significant impairment of growth was noted in culture, sustained, RNAi-mediated inhibition of Axl expression in tumor cells blocked the growth of solid human neoplasms in an *in vivo* MDA-MB-231 human breast cancer xenograft model. This experiment provides functional evidence that Axl signaling may contribute to driving human tumor growth. The recently reported induction of the protumorigenic cytokine interleukin-8 (IL-8) by Axl family RTKs (48) is compatible with a model in which Gas6-Axl signaling enhances tumor growth and supportive angiogenesis in part via the local induction of cytokine secretion. Confluent, serum-deprived MDA-MB-231 cells up-regulate Gas6 message (data not shown) consistent with the finding that these cells produce IL-8 under serum starvation conditions (49). Correspondingly, we have observed expression of human Gas6 in MDA-MB-231 xenograft samples (data not shown).

In addition to angiogenic endothelial cells and neoplastic cells, solid tumors offer perivascular cells as potential cellular therapeutic targets (50). Disruption of pericyte function using platelet-derived growth factor receptor inhibitors synergizes with VEGFR2 inhibition in endothelial cells resulting in enhanced inhibition of angiogenesis and tumor (51). Interestingly, Axl expression is up-regulated in VSMCs of developing blood vessels (31) and Axl-Gas6 signaling plays key roles in activation of SMCs after vascular injury (29). Whereas the function of Axl in pericytes or VSMCs in developing vessels is not established, inhibition of Axl may also potentially disrupt the support function of such perivascular cells providing a third level at which Axl targeting could intervene to suppress tumor growth (Fig. 6). We have recently discovered small-molecule inhibitors of Axl signaling (data not shown). We hypothesize that disruption of Axl signaling using a small-molecule inhibitor may simultaneously affect the endothelial cell, pericyte, and tumor cell compartments, independently targeting angiogenesis and tumor growth and providing a highly effective method to treat solid human tumors.

Acknowledgments

Received 3/24/2005; revised 7/19/2005; accepted 8/4/2005.

The costs of publication of this article were defrayed in part by the payment of page charges. This article must therefore be hereby marked *advertisement* in accordance with 18 U.S.C. Section 1734 solely to indicate this fact.

We thank Hua Wang for statistical analysis.

References

1. Mueller MM, Fusenig NE. Friends or foes: bipolar effects of the tumour stroma in cancer. Nat Rev Cancer 2004;4:839–49.
2. Ridley AJ, Schwartz MA, Burridge K, et al. Cell migration: integrating signals from front to back. Science 2003;302:1704–9.
3. Jain RK. Molecular regulation of vessel maturation. Nat Med 2003;9:685–93.
4. Ferrara N, Gerber HP, LeCouter J. The biology of VEGF and its receptors. Nat Med 2003;9:669–76.
5. Hurwitz H, Fehrenbacher L, Novotny W, et al. Bevacizumab plus irinotecan, fluorouracil, and leucovorin for metastatic colorectal cancer. N Engl J Med 2004; 350:2335–42.
6. Ferrara N, Hillan KJ, Gerber HP, Novotny W. Discovery and development of bevacizumab, an anti-VEGF antibody for treating cancer. Nat Rev Drug Discov 2004;3: 391–400.
7. Lorens JB, Sousa C, Bennett MK, Molineaux SM, Payan DG. The use of retroviruses as pharmaceutical tools for target discovery and validation in the field of functional genomics. Curr Opin Biotechnol 2001;12:613–21.
8. Varnum BC, Young C, Elliott G, et al. Axl receptor tyrosine kinase stimulated by the vitamin K-dependent protein encoded by growth-arrest-specific gene 6. Nature 1995;373:623–6.
9. Stitt TN, Conn G, Gore M, et al. The anticoagulation factor protein S and its relative, Gas6, are ligands for the Tyro 3/Axl family of receptor tyrosine kinases. Cell 1995; 80:661–70.
10. Lorens JB, Jang Y, Rossi AB, Payan DG, Bogenberger JM. Optimization of regulated LTR-mediated expression. Virology 2000;272:7–15.
11. Wakabayashi-Ito N, Nagata S. Characterization of the regulatory elements in the promoter of the human elongation factor-1α gene. J Biol Chem 1994;269:29831–7.
12. Swift SE, Lorens JB, Achacoso P, Nolan GP. Rapid production of retroviruses for efficient gene delivery to mammalian cells using 293T cell-based systems. In: Coligan JE, Kruisbeek AM, Margulies DH, Shevach EM, Strober W, editors. Current protocols in immunology. Vol. 10.17C. New York: John Wiley and Sons, Inc.; 1999. p. 1–17.
13. Henkemeyer M, Marengere LE, McGlade J, et al. Immunolocalization of the Nuk receptor tyrosine kinase suggests roles in segmental patterning of the brain and axonogenesis. Oncogene 1994;9:1001–14.
14. Nor JE, Peters MC, Christensen JB, et al. Engineering and characterization of functional human microvessels in immunodeficient mice. Lab Invest 2001;81:453–63.
15. Perez OD, Kinoshita S, Hitoshi Y, et al. Activation of the PKB/AKT pathway by ICAM-2. Immunity 2002;16: 51–65.
16. Hitoshi Y, Gururaja T, Pearsall DM, et al. Cellular localization and antiproliferative effect of peptides discovered from a functional screen of a retrovirally delivered random peptide library. Chem Biol 2003;10: 975–87.
17. Holland SJ, Liao XC, Mendenhall MK, et al. Functional cloning of Src-like adapter protein-2 (SLAP-2), a novel inhibitor of antigen receptor signaling. J Exp Med 2001;194:1263–76.
18. Kinsella TM, Ohashi CT, Harder AG, et al. Retrovirally delivered random cyclic peptide libraries yield inhibitors of interleukin-4 signaling in human B cells. J Biol Chem 2002;277:37512–8.
19. Chu P, Pardo J, Zhao H, et al. Systematic identification of regulatory proteins critical for T-cell activation. J Biol 2003;2:21.
20. Xu X, Leo C, Jang Y, et al. Dominant effector genetics in mammalian cells. Nat Genet 2001;27:23–9.
21. Pimentel-Muinos FX, Seed B. Regulated commitment of TNF receptor signaling: a molecular switch for death or activation. Immunity 1999;11:783–93.
22. Lorens JB, Bennett MK, Pearsall DM, et al. Retroviral delivery of peptide modulators of cellular functions. Mol Ther 2000;1:438–47.
23. Avanzi GC, Gallicchio M, Bottarel F, et al. GAS6 inhibits granulocyte adhesion to endothelial cells. Blood 1998;91:2334–40.
24. Fridell YW, Villa J, Jr., Attar EC, Liu ET. GAS6 induces Axl-mediated chemotaxis of vascular smooth muscle cells. J Biol Chem 1998;273:7123–6.
25. O'Bryan JP, Frye RA, Cogswell PC, et al. Axl, a transforming gene isolated from primary human myeloid leukemia cells, encodes a novel receptor tyrosine kinase. Mol Cell Biol 1991;11:5016–31.
26. Janssen JW, Schulz AS, Steenvoorden AC, et al. A novel putative tyrosine kinase receptor with oncogenic potential. Oncogene 1991;6:2113–20.
27. McCloskey P, Pierce J, Koski RA, Varnum B, Liu ET. Activation of the Axl receptor tyrosine kinase induces mitogenesis and transformation in 32D cells. Cell Growth Differ 1994;5:1105–17.
28. Meric F, Lee WP, Sahin A, Zhang H, Kung HJ, Hung MC. Expression profile of tyrosine kinases in breast cancer. Clin Cancer Res 2002;8:361–7.
29. Melaragno MG, Fridell YW, Berk BC. The Gas6/Axl system: a novel regulator of vascular cell function. Trends Cardiovasc Med 1999;9:250–3.
30. Neubauer A, Fiebeler A, Graham DK, et al. Expression of axl, a transforming receptor tyrosine kinase, in normal and malignant hematopoiesis. Blood 1994;84: 1931–41.
31. O'Donnell K, Harkes IC, Dougherty L, Wicks IP. Expression of receptor tyrosine kinase Axl and its ligand Gas6 in rheumatoid arthritis: evidence for a novel endothelial cell survival pathway. Am J Pathol 1999;154: 1171–80.
32. Bellosta P, Zhang Q, Goff SP, Basilico C. Signaling through the ARK tyrosine kinase receptor protects from apoptosis in the absence of growth stimulation. Oncogene 1997;15:2387–97.
33. Collett G, Wood A, Alexander MY, et al. Receptor tyrosine kinase Axl modulates the osteogenic differentiation of pericytes. Circ Res 2003;92:1123–9.
34. Lu Q, Gore M, Zhang Q, et al. Tyro-3 family receptors are essential regulators of mammalian spermatogenesis. Nature 1999;398:723–8.
35. van Ginkel PR, Gee RL, Shearer RL, et al. Expression of the receptor tyrosine kinase Axl promotes ocular melanoma cell survival. Cancer Res 2004;64:128–34.
36. Yanagita M. The role of the vitamin K-dependent growth factor Gas6 in glomerular pathophysiology. Curr Opin Nephrol Hypertens 2004;13:465–70.
37. Healy AM, Schwartz JJ, Zhu X, Herrick BE, Varnum B, Farber HW. Gas 6 promotes Axl-mediated survival in pulmonary endothelial cells. Am J Physiol Lung Cell Mol Physiol 2001;280:L1273–81.
38. Angelillo-Scherrer A, Burnier L, Flores N, et al. Role of Gas6 receptors in platelet signaling during thrombus stabilization and implications for antithrombotic therapy. J Clin Invest 2005;115:237–46.

39. Eliceiri BP. Integrin and growth factor receptor crosstalk. Circ Res 2001;89:1104–10.
40. Allen MP, Linseman DA, Udo H, et al. Novel mechanism for gonadotropin-releasing hormone neuronal migration involving Gas6/Ark signaling to p38 mitogen-activated protein kinase. Mol Cell Biol 2002; 22:599–613.
41. Hasanbasic I, Cuerquis J, Varnum B, Blostein MD. Intracellular signaling pathways involved in Gas6-Axl-mediated survival of endothelial cells. Am J Physiol Heart Circ Physiol 2004;287:H1207–13.
42. Hoang MV, Whelan MC, Senger DR. Rho activity critically and selectively regulates endothelial cell organization during angiogenesis. Proc Natl Acad Sci U S A 2004;101:1874–9.
43. Davis GE, Bayless KJ. An integrin and Rho GTPase-dependent pinocytic vacuole mechanism controls capillary lumen formation in collagen and fibrin matrices. Microcirculation 2003;10:27–44.
44. Shiojima I, Walsh K. Role of Akt signaling in vascular homeostasis and angiogenesis. Circ Res 2002; 90:1243–50.
45. Luo J, Manning BD, Cantley LC. Targeting the PI3K-Akt pathway in human cancer: rationale and promise. Cancer Cell 2003;4:257–62.
46. Bellosta P, Costa M, Lin DA, Basilico C. The receptor tyrosine kinase ARK mediates cell aggregation by homophilic binding. Mol Cell Biol 1995;15:614–25.
47. Gallicchio M, Mitola S, Valdembri D, et al. Inhibition of vascular endothelial growth factor receptor 2-mediated endothelial cell activation by Axl tyrosine kinase receptor. Blood 2005;105:1970–6.
48. Wu YM, Robinson DR, Kung HJ. Signal pathways in up-regulation of chemokines by tyrosine kinase MER/NYK in prostate cancer cells. Cancer Res 2004;64:7311–20.
49. Schneider GP, Salcedo R, Welniak LA, Howard OM, Murphy WJ. The diverse role of chemokines in tumor progression: prospects for intervention. Int J Mol Med 2001;8:235–44.
50. Saharinen P, Alitalo K. Double target for tumor mass destruction. J Clin Invest 2003;111:1277–80.
51. Bergers G, Song S, Meyer-Morse N, Bergsland E, Hanahan D. Benefits of targeting both pericytes and endothelial cells in the tumor vasculature with kinase inhibitors. J Clin Invest 2003;111:1287–95.